



Cite this: *Environ. Sci.: Water Res. Technol.*, 2026, 12, 827

## Innovative method for stable operation of low ammonia nitrogen nitrification systems: integrated enhancement strategy

Zongyan Fan,<sup>a</sup> Boru Chen,<sup>b</sup> Salma Tabassum <sup>\*cd</sup> and Tao Xiang<sup>\*a</sup>

This study proposes an integrated strategy combining intermittent aeration, methyl *p*-hydroxy-phenylpropionate (MHPP) with syringic acid (SA), and hydrazine (N<sub>2</sub>H<sub>4</sub>) to address the instability of nitrification in autotrophic nitrogen removal systems treating low-ammonia wastewater. Achieving stable nitrification is critical for efficient autotrophic nitrogen removal in such systems. Yet, it remains challenging due to the difficulty in selectively suppressing nitrite-oxidizing bacteria (NOB) under low ammonia-conditions. Nitrogen transformation patterns and microbial community succession were analyzed by comparing the effects of the two inhibitors with N<sub>2</sub>H<sub>4</sub>. The R1 reactor employing the MHPP + N<sub>2</sub>H<sub>4</sub> + intermittent aeration strategy achieved a nitrite accumulation rate (NAR) of 83.75% in the third phase, with a nitrate accumulation efficiency of only 9.64%. In contrast, the R2 reactor (using SA + N<sub>2</sub>H<sub>4</sub> + intermittent aeration) reached an NAR of only 55.61%, while its nitrate accumulation efficiency exceeded 38.63%. Functional gene prediction revealed a 98% increase in the abundance of the AMO gene in R1 compared to the initial phase, confirming that MHPP selectively inhibits nitrite-oxidizing bacteria (NOB) while promoting the metabolism of ammonia-oxidizing bacteria (AOB). High-throughput sequencing further verified a significant reduction in NOB abundance in the R1 system (0.017%,  $p < 0.01$ ). Microbial community reconstruction revealed that stable system performance was achieved through the synergistic inhibition of NOB and the optimization of the AOB ecological niche. This study offers an innovative approach to stabilize nitrogen removal in low-ammonia wastewater treatment, addressing an urgent need for effective and sustainable solutions under challenging operational conditions.

Received 23rd August 2025,  
Accepted 28th November 2025

DOI: 10.1039/d5ew00814j

rs.li/es-water

### Water impact

Reactive oxygen species, a metabolic byproduct of nitrification inhibitors, are strongly tolerated by ammonia-oxidizing bacteria (AOB), but nitrite-oxidizing bacteria (NOB) lack key genes needed to resist ROS. This study proposes a combined strategy of nitrification inhibitors, N<sub>2</sub>H<sub>4</sub> and intermittent aeration, aiming to achieve rapid start-up and stable operation of the nitrification process. Methyl *p*-hydroxy-phenylpropionate and syringic acid, two biological nitrification inhibitors, were chosen for this study to examine the effects of combining various biological nitrification inhibitors, N<sub>2</sub>H<sub>4</sub>, and intermittent aeration on the stable operation of the low-ammonia nitrogen nitrification system. Combined with functional gene prediction, the influence of the combined strategy's mechanism on the microbial community's function was revealed. It's an innovative method for stable & efficient nitrite production in low-ammonia wastewater systems.

## 1. Introduction

Pursuing novel low-organic-carbon, high-efficiency biological nitrogen removal technologies is necessary due to the high energy consumption, high operating costs, and excess sludge production of traditional biological nitrogen removal processes (nitrification-denitrification).<sup>1</sup> The autotrophic nitrogen removal method, which combines nitrification and anaerobic ammonia oxidation (anammox), has garnered widespread attention because it significantly reduces the energy required for aeration, eliminates the need for an external carbon source,

<sup>a</sup> School of Municipal and Environmental Engineering, Shenyang Jianzhu University, Shenyang 110000, China. E-mail: david76@sjzu.edu.cn; Tel: +905011085451

<sup>b</sup> School of Medicine, Shaanxi International College of Commerce, Xian 710000, China

<sup>c</sup> Department of Chemistry, Faculty of Science, Sakarya University, Sakarya 54187, Türkiye. E-mail: tsalma@sakarya.edu.tr

<sup>d</sup> Biomedical, Magnetic and Semiconductor Materials Research Center (BIMAS-RC), Sakarya University, Sakarya 54187, Türkiye

and has a low excess sludge yield.<sup>2</sup> In the two main phases of complete nitrification, ammonia-oxidizing bacteria (AOB) convert ammonia nitrogen ( $\text{NH}_4^+\text{-N}$ ) to nitrite nitrogen ( $\text{NO}_2^-\text{-N}$ ), which is then oxidized by nitrite-oxidizing bacteria (NOB) to nitrate nitrogen ( $\text{NO}_3^-\text{-N}$ ).<sup>3</sup>

The nitrification process begins with nitritation, primarily providing the required substrate  $\text{NO}_2^-\text{-N}$  for the subsequent anammox process. However, if improperly controlled, NOB can oxidize  $\text{NO}_2^-\text{-N}$  to  $\text{NO}_3^-\text{-N}$ , disrupting autotrophic nitrogen removal. AOB and NOB can destabilize the nitritation process, as they are nitrifying bacterial communities with comparable growth conditions, especially in low  $\text{NH}_4^+\text{-N}$  environments, where NOB readily adapt.<sup>4</sup> Therefore, the key to further overcoming the application bottleneck of autotrophic nitrogen removal technology is to effectively suppress the growth of NOB, thereby achieving stable operation of the nitritation process.

When treating high-concentration  $\text{NH}_4^+\text{-N}$  wastewater, high free ammonia (FA) can form a natural inhibition on NOB, thereby achieving the efficient and stable operation of the autotrophic nitrogen removal process.<sup>5</sup> As autotrophic bacteria, the activity improvement of AOB is limited under low-substrate conditions, and the low FA concentration is insufficient to inhibit NOB for low  $\text{NH}_4^+\text{-N}$  concentrations (20–50  $\text{mg L}^{-1}$ ) in wastewater such as municipal sewage.<sup>6,7</sup> To overcome this challenge, intermittent aeration is a frequently employed control technique that inhibits NOB by taking advantage of AOB's strong affinity for DO.

The recovery of NOB activity during the anoxic-to-aerobic transition is slower than that of AOB, and a proper distribution of anoxic and aerobic time can sustain NOB's low-activity state for extended periods.<sup>8,9</sup> Intermittent aeration and a low DO concentration (0.15  $\text{mg L}^{-1}$ ) during the aerobic phase were used by Ma *et al.*<sup>10</sup> to inhibit NOB activity further. Long-term operation causes NOB to adapt to their environment, gradually disrupting the nitritation process. Researchers have recently investigated several novel techniques to inhibit NOB activity, including the use of blue light irradiation,<sup>11</sup> ultrasonic irradiation,<sup>12</sup> and magnetic field exposure,<sup>13</sup> among others. This research group has also previously performed optimized dosage tests for hydrazine ( $\text{N}_2\text{H}_4$ ). A low  $\text{N}_2\text{H}_4$  concentration can effectively inhibit NOB, however, NOB subsequently adapt to the environment, thereby disturbing the nitritation process again.<sup>14</sup> Although this research has progressed, issues including their high cost and inconsistent inhibitory effects on NOB remain. It is challenging to achieve long-term stable operation of the nitritation process with a single inhibitory strategy.<sup>15</sup>

In current wastewater treatment practices, other strategies for suppressing nitrite-oxidizing bacteria (NOB), such as the application of electric/magnetic fields, maintaining high free ammonia (FA) concentrations, or precise dissolved oxygen (DO) control, often face limitations. These include high operational costs, questionable practical feasibility, significant operational complexities, and the known resilience of NOB. Consequently, utilizing nitrification inhibitors presents a more straightforward and rapid approach (*e.g.*, *via* ROS generation, natural NOB suppression), benefiting from easier availability and

implementation. “Nitrification inhibition” was postulated by Subbarao *et al.*<sup>16</sup> Chemical nitrification inhibitors are compounds synthesized through chemical processes. In contrast, biological nitrification inhibitors (BNIs) are substances that produce and secrete inhibitory effects on nitrification in the root systems of plants in nature.<sup>16</sup> Nitrification inhibitors are widely applied in soil agriculture, but systematic research has not yet been conducted in water treatment.<sup>17</sup>

In preliminary experiments, the research team discovered that different nitrification inhibitors could effectively suppress nitrifying bacteria (NOB) while promoting the activity expression of ammonia-oxidizing bacteria (AOB). Subsequently, a comprehensive preliminary screening was conducted on two significant categories of nitrification inhibitors: chemical nitrification inhibitors and biological nitrification inhibitors (BNIs). This study evaluated the effects of multiple biological nitrification inhibitors on ammonia-oxidizing bacteria (AOB) and nitrifying bacteria (NOB). Comparative assessments revealed that in short-term batch experiments, MHPP and SA demonstrated superior nitrification efficiency. Therefore, SA and MHPP, two biological nitrification inhibitors, were chosen for this study to examine the effects of combining various biological nitrification inhibitors,  $\text{N}_2\text{H}_4$ , and intermittent aeration on the stable operation of the low-ammonia nitrogen nitritation system. While previous studies have investigated the application of hydrazine ( $\text{N}_2\text{H}_4$ ) alone for achieving partial nitrification, our experimental results demonstrate a clear advantage of the proposed synergistic strategy. Key performance indicators, including the nitrite accumulation rate and the relative abundances of AOB/NOB, were significantly higher in our system compared to those reported in studies utilizing  $\text{N}_2\text{H}_4$  solely. Therefore, the synergistic effect proposed in our study is confirmed to be substantial and effective. Moreover, the microbial community's phylum and genus-level succession patterns were examined using high-throughput sequencing technology. In contrast, when combined with functional gene prediction, the influence of the combined strategy on the microbial community's function was revealed.

## 2. Materials and methods

### 2.1. Experimental set-up

The experiment utilized two plexiglass upflow sludge blanket (USB) reactors, with a cylindrical reaction zone (height: 80 cm, inner diameter: 7 cm) and a three-phase separator. The reactors had a total volume of 8.1 L and an effective volume of 5 L.

A 2 cm thick water bath layer (1 L) was externally wrapped and connected to a temperature control system and then covered externally with black insulation material to minimize light exposure. Continuous flow operation was employed, HRT was controlled by peristaltic pumps, and sampling ports were set on both sides to collect samples (Fig. 1).  $\text{NH}_4^+\text{-N}$ ,  $\text{NO}_2^-\text{-N}$ , and  $\text{NO}_3^-\text{-N}$  concentrations in the influent and effluent were monitored daily.

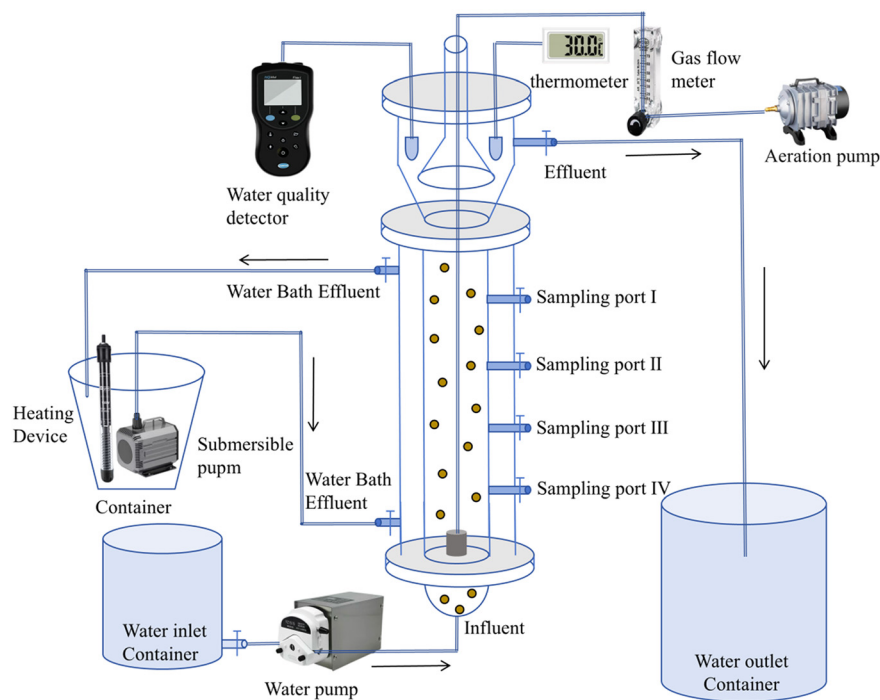


Fig. 1 Schematic design of the reactor unit.

## 2.2. Experimental design

The experiment set up two reactors, with MHPP as the biological inhibitor in R1 and SA as the biological inhibitor in R2. The temperature was kept at  $35 \pm 0.5$  °C, the HRT at 14 h, and the pH between 7.5 and 8.0 during the experiment. Phase I examined how stored sludge affected the low  $\text{NH}_4^+\text{-N}$  nitrification system's ability to operate stably and compared the relative abundances of the bacterial community before and after sludge storage. Phase II investigated the effect of the combined strategy on the startup and steady-state operation of the low  $\text{NH}_4^+\text{-N}$  nitrification system by integrating the biological inhibitor with the stored sludge approach. Phase I and phase II employed an intermittent aeration strategy to control DO (Table 1).

## 2.3. Wastewater composition and inoculated sludge

The synthetic wastewater had the following composition, which was in accordance with the results of Xiang *et al.*<sup>18</sup>  $0.2 \text{ g L}^{-1} \text{ CaCl}_2$ ,  $0.2 \text{ g L}^{-1} \text{ MgSO}_4$ ,  $2 \text{ g L}^{-1} \text{ NaHCO}_3$ ,  $0.025 \text{ g L}^{-1} \text{ KH}_2\text{PO}_4$ , and  $1 \text{ mL L}^{-1}$  trace element solution.<sup>19</sup>

The primary source of  $\text{NH}_4^+\text{-N}$  was ammonium sulfate ( $(\text{NH}_4)_2\text{SO}_4$ ), which had a concentration of  $40 \text{ mg L}^{-1}$ . The

source of the sludge was the nitrifying sludge from the Sanbaotun Sewage Treatment Plant in Fushun City, Liaoning Province, China. After inoculation, the concentrations of mixed liquor suspended solids (MLSS) and mixed liquor volatile suspended solids (MLVSS) were  $4000 \text{ mg L}^{-1}$  and  $2800 \text{ mg L}^{-1}$ , respectively. The sludge samples were settled for 24 hours after collection, and then, the supernatant, suspended heterotrophic bacteria, and impurities were removed.

$\text{NH}_4^+\text{-N}$ ,  $\text{NO}_3^-\text{-N}$ , and  $\text{NO}_2^-\text{-N}$  concentrations were determined according to standard methods.<sup>20</sup> A multiparameter water quality analyzer measured DO, temperature, and pH.

## 2.4. Microbial analysis

DNA samples extracted from the sludge were sequenced on an Illumina MiSeq platform after amplification of the V3–V4 hypervariable region of the 16S rRNA gene using primers 338F and 806R. The raw sequencing data were processed using a standardized bioinformatics pipeline. Quality filtering and assembly of paired-end reads were performed with QIIME and FLASH, respectively. High-quality sequences were clustered into operational taxonomic units (OTUs) at a 97% similarity

Table 1 Experimental design

Stages	Strategy	Bioinhibitor/ $\text{N}_2\text{H}_4$ ( $\text{mg L}^{-1}$ )	Operating time (days)	$\text{NH}_4^+\text{-N}$ ( $\text{mg L}^{-1}$ )
I	Intermittent aeration	0/0	0–15	40
II	Bioinhibitor	5/0	16–36	40
III	Bioinhibitor + $\text{N}_2\text{H}_4$	5/5	37–45	40

threshold using the USEARCH software. Taxonomic assignment was performed using the RDP classifier against the Greengene database at an 80% confidence threshold. Subsequent analyses included microbial community succession and changes in functional abundance. The raw sequence data have been deposited in a public database. The dynamic succession of microbial communities and shifts in the abundance of functional bacterial populations were then examined in detail using the raw sequencing data.

### 2.5. PICRUSt2 analysis

The PICRUSt2 analysis was performed to predict the functional potential of the microbial communities based on the 16S rRNA gene sequencing data. The analysis used PICRUSt2 software (version 2.5.0) with the standard workflow. Briefly, the ASV sequences were placed into a reference phylogeny using `place_seqs.py`. The hidden state prediction algorithm was then applied to infer gene families (KEGG Orthologs) with the `-stratified` option. Finally, metagenome contributions were predicted, and pathway abundances were computed. Default parameters were used for all steps unless otherwise specified, including the default HMMER e-value threshold for sequence placement. This approach provided inferred relative abundances of Kyoto Encyclopedia of Genes and Genomes (KEGG) pathways.

## 3. Results and discussion

### 3.1. Nitrogen transformation in the low- $\text{NH}_4^+$ -N nitrification system under the combined strategy

**3.1.1. Changes in nitrogen elements during R1 operational phases.** The dynamic variations in nitrogen concentrations over time in the R1 reactor are depicted in Fig. 2. The initial influent  $\text{NH}_4^+$ -N concentration was  $40 \text{ mg L}^{-1}$ . The experiment was conducted in three phases for investigation. The reactor operated solely on intermittent aeration without adding MHPP during phase I (1–6 d). On day 6, the  $\text{NH}_4^+$ -N transformational efficiencies were 50.83%, and the  $\text{NO}_2^-$ -N and  $\text{NO}_3^-$ -N accumulated efficiencies were 8.89% and 82.03%, respectively. This suggests that sole DO regulation is insufficient to inhibit NOB activity under low  $\text{NH}_4^+$ -N conditions effectively. Phase II (7–16 days) commenced with the addition of  $5 \text{ mg L}^{-1}$  MHPP to the reactor influent, while intermittent aeration continued as the aeration method. The NAR exhibited an overall rising trend, reaching 42.22% by day 16, while the  $\text{NH}_4^+$ -N transformational efficiency stabilized at approximately 50%. Concurrently, the accumulated efficiencies of  $\text{NO}_3^-$ -N dropped to 58.41%. The findings suggest that although this approach might promote  $\text{NO}_2^-$ -N accumulation to a certain degree, the accumulation effect was relatively limited. Based on this observation, the R1 reactor entered phase III (17–44 d) by adding  $5 \text{ mg L}^{-1}$   $\text{N}_2\text{H}_4$  on top of the phase II regulatory method. The NAR then sharply rose, peaking at 83.75% on day 31 and then remained at 80%. The concentrations of  $\text{NO}_2^-$ -N,  $\text{NH}_4^+$ -N, and  $\text{NO}_3^-$ -N in the effluent were  $17.93 \text{ mg L}^{-1}$ ,  $21.54 \text{ mg L}^{-1}$ , and  $8.04 \text{ mg L}^{-1}$  on day 31. During phase III, the cumulative  $\text{NO}_3^-$ -N efficiencies

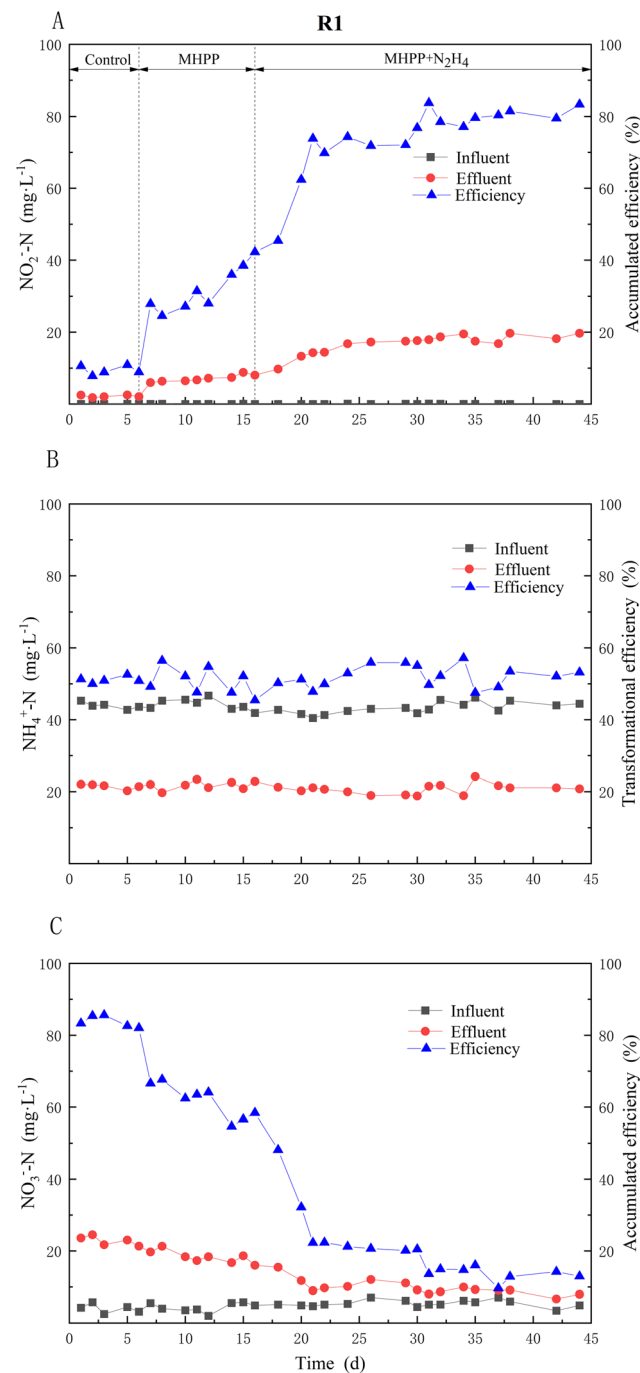


Fig. 2 Variations in nitrogen transformation efficiency during different operational phases of R1: (A)  $\text{NO}_2^-$ -N; (B)  $\text{NH}_4^+$ -N; (C)  $\text{NO}_3^-$ -N.

showed a continual decline trend, falling to at least 9.64%, while the  $\text{NH}_4^+$ -N transformative efficiency continuously remained around  $50 \pm 10\%$ . A comparative analysis reveals that our strategy yields better results than those achieved by the sole addition of  $\text{N}_2\text{H}_4$  (reported NAR:  $65 \pm 5\%$ ) under comparable conditions reported in the literature.<sup>21</sup> These results demonstrate that the NAR is effectively enhanced and the combined control strategy of intermittent aeration, MHPP, and  $\text{N}_2\text{H}_4$  significantly reduces  $\text{NO}_3^-$ -N accumulation. This provides

a synergistic enhancement effect under low  $\text{NH}_4^+\text{-N}$  concentrations. Additionally, the  $\text{NH}_4^+\text{-N}$  transformational efficiency meets the actual requirements of the autotrophic nitrogen removal process.<sup>22</sup>

**3.1.2. Changes in nitrogen elements during R2 operational phases.** The R2 reactor's dynamic nitrogen concentration changes over time are depicted in Fig. 3. The experiment was divided into three phases. During phase I, the experimental data are identical to those of reactor R1.



**Fig. 3** Variations in nitrogen transformation efficiency during different operational phases of R1: (A)  $\text{NO}_2^-\text{-N}$ ; (B)  $\text{NH}_4^+\text{-N}$ ; (C)  $\text{NO}_3^-\text{-N}$ .

Based on intermittent aeration,  $5 \text{ mg L}^{-1}$  SA was added to the reactor during phase II (7–16 d). The NAR peaked on day 15 of this phase at 41.01%, but simultaneously, the accumulated efficiency of  $\text{NO}_3^-\text{-N}$  showed a declining trend, falling to 64.15%. Additionally, the  $\text{NH}_4^+\text{-N}$  transformational efficiency remained approximately 50%. The data changes indicate that  $\text{NO}_2^-\text{-N}$  accumulation was partially achieved, and the  $\text{NH}_4^+\text{-N}$  transformative efficiency progressively met the requirements of the autotrophic nitrogen removal process.<sup>22</sup> Although effective  $\text{NO}_2^-\text{-N}$  accumulation occurred in phase II, further improvement was needed. Therefore,  $5 \text{ mg L}^{-1}$   $\text{N}_2\text{H}_4$  was continually supplied to the R2 reactor during phase III (17–43 days). The NAR rose during this phase, peaking on day 37 at 55.61%. During that period,  $\text{NO}_2^-\text{-N}$ ,  $\text{NH}_4^+\text{-N}$ , and  $\text{NO}_3^-\text{-N}$  effluent concentrations were  $9.03 \text{ mg L}^{-1}$ ,  $26.20 \text{ mg L}^{-1}$ , and  $12.98 \text{ mg L}^{-1}$ , respectively. During this phase, the  $\text{NO}_3^-\text{-N}$  accumulation efficiency dropped to at least 38.63%. Notably, the  $\text{NH}_4^+\text{-N}$  transformative efficiency dropped compared to phases I and II. This could be because the addition of  $\text{N}_2\text{H}_4$  made SA more toxic to AOB.

Based on these findings, the combined strategy of intermittent aeration, SA, and  $\text{N}_2\text{H}_4$  is more effective than any single method in promoting nitrite accumulation. It may effectively promote  $\text{NO}_2^-\text{-N}$  accumulation and substantially increase the NAR. However, it is worth noting that adding SA slightly reduces the transformational efficiency of ammonium nitrogen. The R1 reactor performed better experimentally than the R2 reactor. This means that the nitrification inhibitor MHPP, in conjunction with intermittent aeration and  $\text{N}_2\text{H}_4$  dosage, produced a greater effect on  $\text{NO}_2^-\text{-N}$  accumulation than SA. Notably, the addition of MHPP did not reduce the ammonia nitrogen transformational efficiency.

It is widely acknowledged that aeration is a fundamental requirement for initiating and maintaining partial nitrification, as insufficient dissolved oxygen (DO) will hinder the process.<sup>23</sup> Theoretically, the stoichiometric oxidation of 1 mol of  $\text{NH}_4^+\text{-N}$  to  $\text{NO}_2^-\text{-N}$  consumes 0.75 mol of  $\text{O}_2$ , which translates to a theoretical oxygen demand of approximately  $68.5 \text{ mg L}^{-1}$   $\text{O}_2$  for converting  $40 \text{ mg L}^{-1}$  of  $\text{NH}_4^+\text{-N}$ . However, the observed oxygen deficiency in the system is a dynamic outcome of controlled operational conditions rather than merely a stoichiometric necessity. From the perspective of oxygen mass transfer kinetics, the DO concentration we measure ( $C_L$ ) represents the bulk liquid phase. As AOB consume oxygen for partial nitrification,  $C_L$  decreases, which in turn increases the oxygen concentration gradient ( $C_s - C_L$ ) and drives the oxygen transfer rate from air bubbles. More critically, within the microbial flocs, a significant oxygen concentration gradient exists due to diffusion limitations. The measured  $C_L$  in the bulk liquid is already low; consequently, the actual DO level within the inner layers of the flocs can be substantially lower or even approach zero. This anoxic microenvironment inside the flocs is crucial for selectively suppressing NOB activity, as NOB typically reside in the outer oxygen-rich zone and are more sensitive to

oxygen fluctuations than AOB. Therefore, intermittent aeration is a strategic control measure. It creates a kinetic limitation that exploits the differential oxygen affinity and spatial distribution between AOB and NOB, effectively promoting nitrite accumulation while preventing excessive aeration that would stimulate the growth of NOB. Our study's rationale is that intermittent aeration alone offers limited enhancement to a partial nitrification system. Introducing Biological Nitrification Inhibitors (BNIs) under such aeration conditions allows us to attribute the observed improvement primarily to the BNIs. BNIs cannot achieve significant effects independently without an ongoing partial nitrification process. This has been consistently demonstrated in our group's preliminary batch tests and previous reactor operations; BNIs only enhance the process when the basic conditions for partial nitrification are met. To directly address this comment, we conducted a dedicated batch experiment. The results confirmed that solely adding BNIs without aeration led to an ammonium conversion rate and a nitrite accumulation rate below 10%, which strongly supports our argument.

Indeed, while  $N_2H_4$  alone can achieve partial nitrification, our results clearly demonstrate a superior performance with the synergistic strategy. We observed a marked improvement in the nitrite accumulation rate and AOB/NOB ratio over the systems using  $N_2H_4$  solely, underscoring the effectiveness of our approach.

The risk of  $N_2H_4$  accumulation is negligible, as its potential degradation rate by AnAOB ( $17.67 \text{ mg (g}^{-1} \text{ VSS}^{-1} \text{ h}^{-1})$ ) would remove a typical dose within minutes, consistent with its undetectable level in our effluent. Furthermore, safety concerns are addressed by using stable, non-corrosive hydrazine sulfate powder (diluted to  $<5 \text{ mg L}^{-1} \text{ N}_2\text{H}_4$ ), not the hazardous liquid hydrazine hydrate. Economically, this strategy also offers advantages. Taking a wastewater treatment plant with a daily capacity of 50 000 tons as an example, its operating costs are primarily composed of electricity expenses. The main electricity-consuming units are the lift pump station (with a total power of 365 kW) and the aeration tanks (with a power of 800 kW). Calculated at  $\$0.15 \text{ kWh}^{-1}$  and a 75% equipment utilization rate, their monthly electricity costs are  $\$29\,565$  and  $\$64\,800$ , respectively, totaling  $\$94\,365$ . Compared to conventional denitrification processes, the ammonia stripping process theoretically reduces aeration energy consumption by 62.5%, lowering monthly electricity costs to  $\$35\,387$ . It also eliminates the carbon source costs of  $\$46\,830$  per month required by traditional processes. However, the ammonia stripping process involves the addition of  $N_2H_4 \cdot H_2SO_4$  and MHPP. Calculated at an average dosage concentration of  $5 \text{ mg L}^{-1}$  for both chemicals, the monthly cost for these chemicals amounts to  $\$59\,006$ . Labor costs at the wastewater treatment plant (42 employees) amount to  $\$42\,205$  monthly. Final calculations show that the operating cost of the traditional biological denitrification process is  $\$0.12$  per ton-day, while the new denitrification process costs  $\$0.09$  per ton-day, demonstrating superior economic efficiency.<sup>24</sup>

### 3.2. Characteristics of microbial community succession in the low- $NH_4^+$ -N nitrification system under the combined strategy

#### 3.2.1. Variations in bacterial communities' relative abundance during R1's operational phases.

Fig. 4 illustrates the shifts in the relative abundance of bacterial communities throughout the R1 reactor's operation. The *Proteobacteria* phylum's relative abundance rose from 31.51% in phase I to 34.02% in phase II at the phylum level. This may be because the MHPP addition selectively inhibits phyla linked to nitrification, reducing competition and promoting the proliferation of *Proteobacteria*. The relative abundance of the *Proteobacteria* phylum grew to 35.03% in phase III, demonstrating that the synergistic effect of MHPP and  $N_2H_4$  significantly promoted the enrichment of *Proteobacteria*, aligning with the goal of nitrification system optimization. The relative abundances of the *Bacteroidota* and *Chloroflexi* phyla remained unchanged during the three phases, suggesting that neither tactic increased their abundance. The relative abundance of the *Actinobacteriota* phylum initially decreased from 4.43% in phase I to 3.37% in phase II, suggesting that the addition of MHPP may have slightly inhibited the growth of *Actinobacteria*. In phase III, it rose to 6.21%, indicating that actinobacterial synthesis was stimulated by the reducing environment that  $N_2H_4$  produced. In phase I, the *Patescibacteria* phylum's relative abundance was 3.74%; in phase II, it increased to 4.52%; and in phase III, it dropped to 3.60%. The fact that these bacteria are typically oligotrophic implies that *Patescibacteria* may have gained a transient advantage upon the initial addition of MHPP, but that the subsequent addition of  $N_2H_4$  impeded their growth.<sup>25</sup> The *Nitrospirota* phylum's relative abundance steadily declined during the first three stages, falling to 2.75% in phase I, 1.03% in phase II, and 0.25% in phase III. This is the result of the combined action of MHPP and  $N_2H_4$ , indicating that this joint strategy played a crucial role in the low



Fig. 4 Distribution of the microbial community in the R1 reactor.

$\text{NH}_4^+$ -N nitrification system by effectively inhibiting the growth of nitrifying bacteria.

*Nitrosomonas* rose from 0.775% to 0.926% at the genus level, whilst *Nitrospira* sharply declined from 0.745% to 0.201% ( $p < 0.001$ ). This suggests that AOB abundance rose while NOB was successfully suppressed following the addition of MHPP. This indicates that AOB abundance increased while NOB was effectively inhibited by the addition of MHPP. Being a biological nitrification inhibitor, MHPP<sup>26</sup> reduced the transformation of  $\text{NO}_2^-$ -N to  $\text{NO}_3^-$ -N by selectively inhibiting NOB activity, thereby promoting  $\text{NO}_2^-$ -N accumulation.

*Nitrosomonas* then grew to 0.954% while *Nitrospira* continued to decrease to 0.017% due to the continuous addition of  $\text{N}_2\text{H}_4$  during the transition from phase II to phase III. In this case,  $\text{N}_2\text{H}_4$  may play two roles: firstly, acting as a reducing agent to further reduce  $\text{NO}_3^-$ -N, decreasing its accumulation. It may also inhibit nitrate reductase activity, further restricting the metabolic activities of NOB.<sup>18</sup>  $\text{N}_2\text{H}_4$  and MHPP had a strong synergistic effect, as evidenced by the nearly complete inhibition of NOB abundance and the continued rise in AOB abundance.

**3.2.2. Variations in bacterial communities' relative abundance during R2 operational phases.** Fig. 5 illustrates the variations in the relative abundance of bacterial communities during the operating stages of the R2 reactor. The *Proteobacteria* phylum's relative abundance rose from 31.51% in phase I to 33.44% in phase II at the phylum level. This may be because SA addition selectively inhibits phyla linked to nitrification, thereby reducing competition and promoting the proliferation of *Proteobacteria*.<sup>27</sup> *Proteobacteria*'s relative abundance dropped to 32.01% in phase III, presumably due to several bacterial groups being adversely affected by the addition of  $\text{N}_2\text{H}_4$ . The relative abundance of the *Bacteroidota* phylum remained essentially unchanged during the three periods, suggesting that neither strategy significantly enhanced its abundance. The relative abundance of the *Chloroflexi* phylum rose dramatically from 9.57% in phase I to 12.93% in phase II, most likely due to the inhibition of other bacterial groups by SA addition, which

allowed the *Chloroflexi* to occupy additional ecological niches. In phase III, it dropped significantly to 8.92% ( $p < 0.01$ ), indicating that the addition of  $\text{N}_2\text{H}_4$  might have changed metabolic pathways and inhibited its growth.

The relative abundance of the *Actinobacteriota* phylum increased steadily throughout the three phases, from 4.43% to 5.34%, indicating that these strategies promoted actinobacterial synthesis or inhibited competing phyla. The *Patescibacteria* phylum's relative abundance rose from 3.74% in phase I to 4.52% in phase II before falling to 3.04% in phase III. This may be because  $\text{N}_2\text{H}_4$  hindered the growth of oligotrophic bacteria by changing environmental conditions, whereas SA inhibited dominant bacterial groups, allowing them to proliferate temporarily. During phase I, the relative abundance of the *Nitrospirota* phylum was 2.75%; in phase II, it dropped to 1.12%; and in phase III, it further declined to 0.76%.

This demonstrates that the combined strategy inhibited the nitrifying bacterial population, effectively promoting stable nitrification operation. The *Nitrosomonas* genus' relative abundance rose from 0.775% in phase I to 1.442% in phase II and 1.554% in phase III at the genus level. This suggests that the inclusion of SA either promoted or did not impede the growth of AOB. *Nitrospira* dropped from 0.745% to 0.110% and then to 0.049%, indicating that SA successfully inhibited NOB.  $\text{N}_2\text{H}_4$  further strengthened this inhibitory effect.

**3.2.3. Microbial community shifts under MHPP and SA inhibition.** Analysis of microbial community succession revealed distinct shifts in response to the different inhibitor strategies. At the phylum level, the key nitrification-associated phylum *Proteobacteria* was more abundant in reactors employing the MHPP-based strategy (C1: 34.02%; C3: 35.03%) compared to those with SA (C2: 33.44%; C4: 32.01%), suggesting a more favorable niche for nitrifying bacteria. A more pronounced difference was observed in the abundance of *Chloroflexi*, which was significantly lower in MHPP systems (C1: 9.80%; C3: 9.78%) compared to SA systems (C2: 12.93%; C4: 8.92%), suggesting that MHPP had a lower impact on organic matter degradation pathways. Furthermore, the SA system exhibited a higher abundance of the *Actinobacteriota* phylum (C2: 5.08%; C4: 5.34%), which can negatively impact nitrification stability by impeding AOB activity. The proliferation of the oligotrophic phylum *Patescibacteria* was also more limited under MHPP treatment, indicating less community disturbance. Crucially, the relative abundance of the NOB-containing phylum *Nitrospirota* was substantially lower in the MHPP +  $\text{N}_2\text{H}_4$  reactor (C3: 0.25%) than in the SA +  $\text{N}_2\text{H}_4$  reactor (C4: 0.76%), demonstrating a superior inhibitory effect on NOB. This differential inhibition was corroborated at the genus level. The abundance of the AOB genus *Nitrosomonas* was enriched in the MHPP +  $\text{N}_2\text{H}_4$  system (C3: 1.55%) compared to its SA counterpart (C4: 0.95%). Concurrently, the critical NOB genus *Nitrospira* was almost completely suppressed in the MHPP +  $\text{N}_2\text{H}_4$  system (C3: 0.02%), achieving a lower level than in the SA +  $\text{N}_2\text{H}_4$  system (C4: 0.05%) and outperforming inhibition levels reported in previous studies using  $\text{N}_2\text{H}_4$  alone. In summary, the combined strategy of intermittent aeration with MHPP and



Fig. 5 Distribution of the microbial community in the R2 reactor.



Fig. 6 Microbial community distribution during the inhibitor stage. C1: intermittent aeration + MHPP; C2: intermittent aeration + SA. C3: intermittent aeration + MHPP + N<sub>2</sub>H<sub>4</sub>; C4: intermittent aeration + SA + N<sub>2</sub>H<sub>4</sub>.

N<sub>2</sub>H<sub>4</sub> established a microbial community structure that was more conducive to the enrichment of AOB while achieving more complete suppression of NOB, thereby proving more effective in stabilizing the nitrification process (Fig. 6).

According to the sequencing data, the only NOB genus detected was Nitrospira. In contrast, other NOB taxa such as Nitrobacter, Nitrotoga, and comammox species (including *Candidatus Nitrospira nitrosa*, *Candidatus Nitrospira nitrificans*, and *Candidatus Nitrospira inopinata*) were not detected. The literature suggests that Nitrotoga are often found in environments with high free ammonia. At the same time, comammox organisms tend to thrive under oligotrophic conditions—neither of which aligns with the experimental conditions in this study. In addition, both our previous research and published reports indicate that Nitrospira are often the dominant NOB in actual wastewater treatment plants and synthetic wastewater systems, occupying a broader ecological niche than Nitrobacter. Therefore, we consider the detection result to be reasonable.

### 3.3. Functional gene analysis

PICRUSt2 can predict the functional composition of microbial communities in samples by analyzing amplicon sequencing data. Based on the obtained microbial sequencing data,

PICRUSt2 was used for the functional analysis of functional bacterial populations to derive the relative abundance of different functional genes, especially those closely related to the autotrophic nitrogen removal pathway.<sup>28</sup> The nitrogen cycle mechanism in the autotrophic nitrogen removal process is depicted in Fig. 7, which also explains the functions of these functional genes.

Fig. 8 illustrates the predicted relative abundance of functional genes related to the nitrification process in R1 and R2 reactors during various treatment phases. The findings show that phase C3 had the highest relative abundance of AMO, at 0.0097%, 98% more than phase C0. This indicates that the synergistic effect of MHPP and N<sub>2</sub>H<sub>4</sub> enhanced the activation of AOB gene expression, leading to a better promotion of AOB functional genes. The relative abundance of HAO closely synchronized with AMO, indicating overall activation of the AOB metabolic pathway. N<sub>2</sub>H<sub>4</sub> may further enhance the hydroxylamine oxidation capacity of AOB by optimizing the substrate environment. The increase in HAO abundance indicates the effective operation of the nitrification process.<sup>18</sup> Because of the exceptionally high NOB activity in the original sludge (as noted in the NXR abundance of 0.0169% in C0), it was challenging for traditional intermittent aeration to inhibit NOB effectively. NXR abundance was dramatically decreased by the addition of

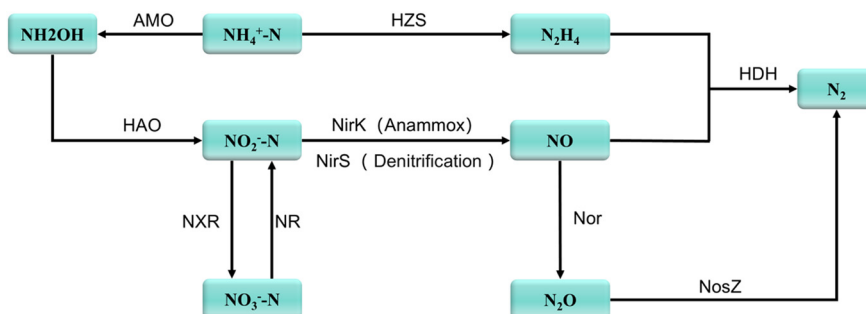


Fig. 7 Schematic diagram of the autotrophic nitrogen removal process, its position in the nitrogen cycle, and the associated functional genes.



**Fig. 8** Changes in the relative abundance of major functional genes of R1 and R2. C0: intermittent aeration; C1: intermittent aeration + MHPP; C2: intermittent aeration + SA; C3: intermittent aeration + MHPP + N<sub>2</sub>H<sub>4</sub>; C4: intermittent aeration + SA + N<sub>2</sub>H<sub>4</sub>.

both MHPP and SA, indicating that both inhibitors successfully inhibited NOB. NXR abundance subsequently declined upon additional combination with N<sub>2</sub>H<sub>4</sub>, with C3 showing the most decrease. NirS/NirK abundance showed minimal variation across phases, indicating that the system was primarily dependent on nitrification with only a moderate denitrification contribution, which is in line with the characteristics of the Partial Nitrification/Anammox (PN/A) process.

NR was undetected throughout the experiment, indicating that dissimilatory nitrate reduction did not occur within the system, with nitrogen removal solely dependent on the PN/A pathway. It has been demonstrated that the oxidation pathway of NO<sub>2</sub><sup>-</sup>-N was successfully inhibited, allowing the nitrification process to operate steadily, combined with the changes and relative abundances of NAR and functional bacterial populations.

### 3.4. Mechanisms of MHPP and SA on AOB and NOB

Based on functional gene and microbial community analyses, MHPP and SA exert distinct inhibitory mechanisms on AOB and NOB, particularly in terms of metabolic targeting and ROS-mediated toxicity. The selective inhibition profile of MHPP suggests a mechanism that predominantly impedes the NXR complex in NOB, thereby blocking nitrite oxidation, while largely sparing the AMO pathway of AOB. This functional selectivity between the two nitrifying groups is a recognized characteristic of certain biological nitrification inhibitors.<sup>29</sup> This is consistent with the distinct metabolic outcomes observed in our system for MHPP. This enzymatic selectivity allows AOB to maintain high metabolic activity and AMO gene expression, as demonstrated by the 98% increase in AMO abundance in MHPP-amended reactors. In contrast, SA exhibits broader metabolic interference, likely through non-specific binding to metalloenzymes involved in both ammonia and nitrite oxidation, which suppresses NOB and partially impairs AOB activity, especially under N<sub>2</sub>H<sub>4</sub> synergy.

Furthermore, the two inhibitors differentially influence intracellular ROS homeostasis. MHPP appears to mitigate oxidative stress in AOB by supporting the upregulation of key antioxidant enzymes, such as superoxide dismutase (SOD) and catalase, thereby enhancing their resilience under intermittent aeration.<sup>26</sup> This is consistent with the observed enrichment of *Nitrosomonas* and elevated HAO gene expression under MHPP treatment. In contrast, SA may exacerbate ROS accumulation within microbial cells due to its phenolic structure, resulting in increased lipid peroxidation and protein damage. While NOB—especially *Nitrospira*—are more susceptible to such oxidative injury, AOB also experience metabolic compromise under prolonged SA exposure, as reflected by the decline in ammonium transformation efficiency. Such mechanistic divergence highlights the ecological and operational benefits of MHPP in maintaining nitrification stability under low-ammonia conditions.

## 4. Conclusion

The MHPP + N<sub>2</sub>H<sub>4</sub> combination performed optimally in dynamic operation during the study's investigation of synergistic enhancement of its combined strategy under intermittent aeration. It achieved a NO<sub>2</sub><sup>-</sup>-N accumulated efficiency of up to 83.75%, decreased the NO<sub>3</sub><sup>-</sup>-N accumulation efficiency to 9.64%, and maintained a stable ammonia nitrogen transformation rate of approximately 50%. *Nitrosomonas* abundance rose to 0.954% whereas *Nitrospira* decreased from 0.745% to 0.017%, indicating that NOB genera were successfully inhibited. Although the SA + N<sub>2</sub>H<sub>4</sub> group promoted AOB enrichment to some extent, its inhibitory effect on NOB was inferior to that of MHPP. The ammonia nitrogen transformative rate dropped to 40%, indicating that adding SA may have an antagonistic impact on N<sub>2</sub>H<sub>4</sub>, affecting the system's stability. According to functional gene prediction, the MHPP + N<sub>2</sub>H<sub>4</sub> strategy favors the long-term stable operation of the low-NH<sub>4</sub><sup>+</sup>-N nitrification system by efficiently suppressing NXR expression while also significantly activating the expression of AMO and HAO genes.

## Author contributions

Zongyan Fan and Boru Chen participated in the design and operation of experiments, writing-original draft, and data analysis. Salma Tabassum and Tao Xiang were responsible for writing-review & editing, proofreading and theoretical derivation, and supervision.

## Conflicts of interest

There are no conflicts to declare.

## Data availability

The authors confirm that the data supporting the findings of this study are available within the article.

## Acknowledgements

This research was supported by the Research Project of Liaoning Provincial Department of Education (No. JYTQN2023395) and Liaoning Province Science and Technology Plan Joint Program (No. 2024-BSLH-237).

## References

- 1 L. Wu, Z. Li, S. Huang, M. Shen, Z. Yan, J. Li and Y. Peng, Low energy treatment of landfill leachate using simultaneous partial nitrification and partial denitrification with anaerobic ammonia oxidation, *Environ. Int.*, 2019, **127**, 452–461.
- 2 T. Xiang, H. Liang and D. Gao, Comparison of recovery characteristics between AnAOB and AOB-AnAOB granular sludge after long-term storage, *Sci. Total Environ.*, 2022, **802**, 149741.
- 3 K. Anna, N. Yury, G. Vladimír, B. Alexey, G. Evgeny, K. Vitaly, D. Alexander, B. Julia, P. Anna, Z. Ivar, R. Nikolai, P. Nikolai and M. Andrey, New Insight Into the Interspecies Shift of Anammox Bacteria Ca. “Brocadia” and Ca. “Jettenia” in Reactors Fed With Formate and Folate, *Front. Microbiol.*, 2022, **12**, 802201.
- 4 C. S. Pitol, A. T. Fernandes, C. G. Menegon, G. P. A. Carneiro, L. G. Bicelli, V. Cano and T. S. O. d. Souza, Enhancing deammonification in a membrane-aerated biofilm reactor: Intermittent aeration and ammonia loading rate control as key strategies for NOB inhibition in low-strength nitrogen wastewater, *J. Water Process Eng.*, 2025, **79**, 108861.
- 5 S. Park and W. Bae, Modeling kinetics of ammonium oxidation and nitrite oxidation under simultaneous inhibition by free ammonia and free nitrous acid, *Process Biochem.*, 2009, **44**, 631–640.
- 6 J. Li, Y. Peng, L. Zhang, J. Liu, X. Wang, R. Gao, L. Pang and Y. Zhou, Quantify the contribution of anammox for enhanced nitrogen removal through metagenomic analysis and mass balance in an anoxic moving bed biofilm reactor, *Water Res.*, 2019, **160**, 178–187.
- 7 J. Gu, M. Zhang, S. Wang and Y. Liu, Integrated upflow anaerobic fixed-bed and single-stage step-feed process for mainstream deammonification: A step further towards sustainable municipal wastewater reclamation, *Sci. Total Environ.*, 2019, **678**, 559–564.
- 8 Y. Miao, L. Zhang, Y. Yang, Y. Peng, B. Li, S. Wang and Q. Zhang, Start-up of single-stage partial nitrification-anammox process treating low-strength swage and its restoration from nitrate accumulation, *Bioresour. Technol.*, 2016, **218**, 771–779.
- 9 G. Wang, X. Xu, Z. Gong, F. Gao, F. Yang and H. Zhang, Study of simultaneous partial nitrification, ANAMMOX and denitrification (SNAD) process in an intermittent aeration membrane bioreactor, *Process Biochem.*, 2016, **51**, 632–641.
- 10 B. Ma, P. Bao, Y. Wei, G. Zhu, Z. Yuan and Y. Peng, Suppressing Nitrite-oxidizing Bacteria Growth to Achieve Nitrogen Removal from Domestic Wastewater via Anammox Using Intermittent Aeration with Low Dissolved Oxygen, *Sci. Rep.*, 2015, **5**(1), 13048.
- 11 K. Kim and Y.-G. Park, Light as a Novel Inhibitor of Nitrite-Oxidizing Bacteria (NOB) for the Mainstream Partial Nitrification of Wastewater Treatment, *Processes*, 2021, **9**(2), 346.
- 12 S. Huang, Y. Zhu, J. Lian, Z. Liu, L. Zhang and S. Tian, Enhancement in the partial nitrification of wastewater sludge via low-intensity ultrasound: Effects on rapid start-up and temperature resilience, *Bioresour. Technol.*, 2019, **294**, 122196.
- 13 Z. Wang, X. Liu, S.-Q. Ni, J. Zhang, X. Zhang, H. A. Ahmad and B. Gao, Weak magnetic field: A powerful strategy to enhance partial nitrification, *Water Res.*, 2017, **120**, 190–198.
- 14 K. Klein, E. Kattel, A. Goi, A. Kivi, N. Dulova, A. Saluste, I. Zekker, M. Trapido and T. Tenno, Combined Treatment of Pyrogenic Wastewater From Oil Shale Retorting, *Oil Shale*, 2017, **34**, 82–96.
- 15 A. A. Nikitina, A. Y. Kallistova, D. S. Grouzdev, T. Y. V. Kolganova, A. A. Kovalev, D. A. Kovalev, V. Panchenko, I. Zekker, A. N. Nozhevnikova and Y. V. Litt, Syntrophic Butyrate-Oxidizing Consortium Mitigates Acetate Inhibition through a Shift from Acetoclastic to Hydrogenotrophic Methanogenesis and Alleviates VFA Stress in Thermophilic Anaerobic Digestion, *Appl. Sci.*, 2022, **13**(1), 173.
- 16 G. V. Subbarao, T. Ishikawa, O. Ito, K. Nakahara, H. Y. Wang and W. L. Berry, A bioluminescence assay to detect nitrification inhibitors released from plant roots: a case study with *Brachiaria humidicola*, *Plant Soil*, 2006, **288**, 101–112.
- 17 Y. Li, Y. Zhang, S. J. Chapman and H. Yao, Biological nitrification inhibition by sorghum root exudates impacts ammonia-oxidizing bacteria but not ammonia-oxidizing archaea, *Biol. Fertil. Soils*, 2021, **57**, 399–407.
- 18 T. Xiang, D. Gao and X. Wang, Performance and microbial community analysis of two sludge type reactors in achieving mainstream deammonification with hydrazine addition, *Sci. Total Environ.*, 2020, **715**, 136377.
- 19 X. Wang and D. Gao, The transformation from anammox granules to deammonification granules in micro-aerobic system by facilitating indigenous ammonia oxidizing bacteria, *Bioresour. Technol.*, 2018, **250**, 439–448.
- 20 I. V. Carranzo, Standard methods for the examination of water and wastewater, *Choice Rev. Online*, 2012, **49**(12), 49–6910.
- 21 Y. Sun, Y. Ma, Y. Cao, S. Liu, X. Tian and B. Dai, Nitrogen removal performance and changes in microbial community structure of a single-stage partial nitrification-anammox (PNA) process for treating municipal wastewater with an extremely low carbon-to-nitrogen ratio, *J. Water Process Eng.*, 2025, **70**, 106931.
- 22 S. Wu, F. Gao, C. Lin, Y. Quan, Y. Wei, Z. Liu, H. Yu, E. H. Sanjaya, M. F. M. Din and H. Chen, A critical review of

- oxygen supply and control strategies in single-stage partial nitrification-anammox system for autotrophic nitrogen removal from wastewater, *J. Environ. Chem. Eng.*, 2025, **13**, 117613.
- 23 S. Abasi, S. Tarre and M. Green, The effect of free ammonia, free nitrous acid, dissolved oxygen and salinity on hypersaline nitrification stability, *Chemosphere*, 2025, **385**, 144576.
- 24 X. Tao, L. Hong and G. Dawen, Effect of exogenous hydrazine on metabolic process of anammox bacteria, *J. Environ. Manage.*, 2022, **317**, 115398.
- 25 E. G. W. Gunawardana, T. J. Sotelo, K. Oshima, M. Hattori, T. Mino and H. Satoh, Categorization of Bacteria That Leak from Activated Sludge to Secondary Treated Water: Year-round Observations, *Microbes Environ.*, 2025, **40**(1), ME24082.
- 26 T. Lan, M. Li, X. He, J. Yuan, M. Zhou, X. Tang, Y. Zhang, Y. Li, Z. Tian and X. Gao, Effects of exogenous carbon and nitrification inhibitors on denitrification rate, product stoichiometry and nirS/nirK-type denitrifiers in a calcareous soil: evidence from 15 N anaerobic microcosm assays, *J. Soils Sediments*, 2023, **23**, 1217–1232.
- 27 Y. Lu, X. Zhang, M. Ma, W. Zu, H. J. Kronzucker and W. Shi, Syringic acid from rice as a biological nitrification and urease inhibitor and its synergism with 1,9-decanediol, *Biol. Fertil. Soils*, 2021, **58**, 277–289.
- 28 P. Xu, Z. Xie, L. Shi, X. Yan, Z. Fu, J. Ma, W. Zhang, H. Wang, B. Xu and Q. He, Distinct responses of aerobic granular sludge sequencing batch reactors to nitrogen and phosphorus deficient conditions, *Sci. Total Environ.*, 2022, **834**, 155369.
- 29 W. V. Macêdo, J. S. Madsen, P. Schacksen, R. Sandeep, J. L. Nielsen, P. Biller and L. Vergeynst, Aerobic biological treatment of hydrothermal liquefaction process water of sewage sludge: Nitrification inhibition and removal of hazardous pollutants, *Water Res.*, 2025, **277**, 123351.